Equation Chapter 1 Section 1EURODYN 2020
Equation Chapter 1 Section 1XI International Conference on Structural Dynamics
M. Papadrakakis, M. Fragiadakis, C. Papadimitriou (eds.)
Athens, Greece, 23–25 November 2020

SHEAR STRENGTHENING OF MASONRY PANELS USING A GFRP-REINFORCED MORTAR COATING

G. Castori[1], E. Speranzini[1], M. Corradi[1,2], S. Agnetti[3] and G. Bisciotti[3]

[1] University of Perugia, Dept. of Engineering
Via Duranti 92, 05100, Perugia Italy
e-mail: giulio.castori@unipg.it emanuela.speranzini@unipg.it

[2] Northumbria University, Dept. of Mechanical & Construction Engineering
Wynne-Jones Building, NE1 8ST Newcastle Upon Tyne, United Kingdom
e-mail: marco.corradi@northumbria.ac.uk

[3] Kimia ltd., Ponte Felcino, 06134 Perugia, Italy
e-mail: stefano.agnetti@kimia.it giordano@kimia.it

Keywords: Conservation engineering, Shear walls, Retrofit, Composite materials

Abstract. *The use of new composite materials for reinforcement of heritage masonry structures, especially in seismic prone areas, is of interest structural engineers and conservators. However, the need to increase the structural performance of masonry structures is often in contrast with the principles of conservation in terms of reversibility, limited visual impact, compatibility of new materials with masonry. With the aim at striking a balance between structural safety and heritage protection, this paper investigates strengthening stone and brickwork masonry walls using glass-fiber reinforced polymer (GFRP) meshes embedded into a coating of lime or cement mortar. An experimental research program was undertaken in the laboratory on large-scale wall panels. Both clay brick and stone work specimens were tested, with and without strengthening. Single-sided and double-sided strengthenings were considered, as it is often not practicable to apply the reinforcement to both sides of a wall. Static tests were carried out on twelve masonry panels, under in-plane diagonal shear loading. The mechanisms by which load was carried were observed, varying from the initial, uncracked state, to the final, fully cracked state. The results demonstrate that a significant increase of the in-plane shear capacity of masonry can be achieved by using the proposed retrofitting technique. The experimental data were used to assess the effectiveness of the strengthening, and a finite element (FE) numerical model is discussed and calibrated against experimental results. The FE model was used to investigate further aspects of the reinforced masonry under shear-loading.*

1 INTRODUCTION

The performance of historic and heritage masonry buildings during previous earthquakes in Italy and other parts of Europe has demonstrated that many structural failures could be attributed to inadequate shear capacity of their wall panels [1, 2, 3]. This was particularly serious not only for very old ashlar stone masonry buildings, but also for those buildings, often more recently built, made of brickwork masonry [4]. The use of very weak lime mortar in construction and inadequate construction methods, not fulfilling the so-called "rules of the art" as defined in historic manuals and recent studies constitute the primary reasons for poor performance.

While it is not socially and economically acceptable to demolish these unsafe buildings, it is possible to retrofit them. A large portion of its programmed economic stimulus in Italy is associated with upgrading the building stock through, for instance schemes for improvement of structural safety of old masonry buildings against the seismic loading (Fig. 1). The anticipated cost benefit of lightweight composite reinforcements that can be easily transported and applied without interfering with the use of the buildings, against the conventional steel/concrete, are presented in Table 1. This table also reports the grade of reversibility and compatibility for different traditional and innovative retrofitting methods for shear walls [5, 6].

Reinforcement method	Brickwork masonry	Stone work masonry	Grade of structural efficiency	Reversibility of intervention	Compatibility with masonry
Lime grout injections	Unsuitable	Suitable/ Unsuitable*	High	Low	Good
Deep repointing of mortar joints with lime new mortar	Suitable/ Unsuitable*	Suitable/ Unsuitable*	Low to Medium	High	Very Good
Epoxy-bonded FRP jacketing	Suitable	Suitable	High	Low	Very Low
Reinforced Concrete Jacketing	Suitable	Suitable	Very High	Low	Very Low
FRCM Jacketing	Suitable	Suitable	Medium to High	High	Good

* highly depends on the masonry type, dimensions the mortar joints, if there are internal voids in the shear walls

Table 1: Reinforcement of shear walls: commercially available methods.

During the past two decades applications of Fiber Reinforced Polymer (FRP) products have increased significantly, most notably for seismic retrofitting. Among many beneficial characteristics of FRP materials are light weight, ease of installation, high tensile strength, and immunity to corrosion [7, 8, 9].

With regard to shear walls, it is well known that FRP jackets can provide additional shear capacity, confinement and clamping force within wall leaves, enhancing wall performance especially when stressed by the action of an earthquake. However, serious limitations remain for the use of epoxy adhesives. These resins are typically employed to fix the composite reinforcements to masonry. Their long term behavior, as well their "compatibility" with masonry materials and the limited "reversibility" of these interventions are object of debate in the scientific community [10]. Conservation bodies often do not authorize the use of epoxy-bonded

FRPs on listed masonry buildings and different retrofitting solutions have been recently proposed.

Figure 1: Examples of different methods to retrofit shear walls: a. Epoxy-bonded Carbon FRP, b. Steel mesh reinforced concrete jacketing, c. Grout Injection in the internal core of multi-leaf stone walls.

The most important Italian Conservation Body (*Soprintendenza Archeologia, Belle Arti e Paesaggio*) supervises around 9.66 M heritage items (archeological sites, heritage buildings and museum assets) with a density of about 33.3 items/100 km^2. In Italy, the density of this enormous quantity of assets is much higher in seismic prone areas (Tuscany, Campania, Marche and Umbria have a density of 40, 41, 49 and 53 items/100 km^2, respectively). In this situation, to overcome the limitations of the use of epoxy-bonded reinforcement, the use of inorganic, i.e. lime or cement based, coatings reinforced with composites meshes has been proposed. The final result is a Fiber Reinforced Cementitious Mortar (FRCM) [11, 12, 13]: this can be easily used to create a jacket, to apply to one or both surfaces of the shear walls. Low fire resistance of FRPs is an issue that can be resolved by using FRCMs: composite materials are embedded in the mortar jacketing and this can also protect the reinforcement.

To verify the effectiveness of FRCM reinforcement with respect to real-scale laterally loaded wall panels, to study the structural behaviour of FRCM reinforced members and to investigate some specific aspects of the modelling of shear walls, shear tests on large-scale panels reinforced with FRCM have been performed. The variables considered in this test program included masonry type, single-side and double-side reinforcement, and method of application of the reinforcement (preventive method, i.e. reinforcement applied to un-cracked walls, or repair method, i.e. reinforcement used to repair damaged or cracked shear walls). Combined experimental and analytical research is underway at the Structures Laboratory of the University of Perugia to investigate the effectiveness of FRCM jackets on the seismic performance of shear walls. Some preliminary results on shear walls tested under simulated seismic loading are presented in the paper. Analytical research, leading to a seismic design approach is also presented. Design performance levels are compared with experimentally obtained drift capacities, verifying the applicability of the design procedure.

2 EXPERIMENTAL VALIDATION

2.1 Wall geometry and test method

The specimens in this study are twelve full-scale shear walls, made of solid bricks or ashlar stone blocks. The walls are 1200 x 1200 mm. The nominal thickness of the brick and stone walls was 240 mm. Thus, all the test specimens had been constructed at once by an expert mason at the Structures Laboratory (Lastru) of the University of Perugia, located in Terni, Italy.


a.


b.

Figure 2:Realization of full-scale shear walls: a. Solid bricks test specimens, b. shear test setup.

Figure 2 shows the test setup: the shear wall panel is subjected to a diagonal, compressive, in-plane loading and fails by a diagonal shear crack, typically originating from the panel's centroid where the stresses are maximum. A highly strained region is assumed to form in the panel's centre at the crack location.

Hence for a linear elastic membrane under in-plane loading, the plane-stress components σ_{xx}, σ_{xy} and σ_{yy} at the panel's centroid are given by:

$$\sigma_{xx} = \sigma_{yy} = -0.56\frac{F}{A_n}$$
$$\sigma_{xy} = \sigma_{yx} = 1.05\frac{F}{A_n}$$

where F is the diagonal force and A_n is the wall horizontal cross section.

The principal stresses σ_I and σ_{II} are:

$$\sigma_I = 0.50\frac{F}{A_n}$$
$$\sigma_{II} = -1.62\frac{F}{A_n} \quad (2)$$

According to the interpretation provided by the RILEM guidelines (Fig. 3), at failure ($F=F_{max}$), σ_I is equal to the masonry tensile strength f_t:

$$f_t = \sigma_I = 0.50 \frac{F_{max}}{A_n} \tag{3}$$

The masonry shear strength, τ_0, at failure, is then given by:

$$\tau_0 = \frac{f_t}{1.5} \tag{4}$$

The two sides of each wall panel have been labelled with letters A and B. Contact instrumentation (LVDT: Linear Variable Differential Transformers) was used to measure the deformation of the panels along the unloaded (in tension) and loaded (in compression) wall's diagonals. The change in length of the wall's diagonal in compression (Δl_{CSA} and Δl_{CSB} for side A and B of the wall panel, respectively) and in tension (Δl_{TSA} and Δl_{TSB}), are giving the compressive and tension strains as:

$$\begin{aligned} \varepsilon_{CSA} &= \frac{\Delta l_{CSA}}{l_{CSA}} \qquad & \varepsilon_{TSA} &= \frac{\Delta l_{TSA}}{l_{TSA}} \\ \varepsilon_{CSB} &= \frac{\Delta l_{CSB}}{l_{CSB}} \qquad & \varepsilon_{TSA} &= \frac{\Delta l_{TSA}}{l_{TSA}} \end{aligned} \tag{5}$$

where l_{CSA} and l_{CSB} are the gage lengths of the LVDTs applied along the compressed diagonals on side A and B, respectively. Similarly, l_{TSA} and l_{TSB} are the gage lengths for the stretched wall diagonals. Hence, the compressive and tensile axial strains, ε_c and ε_t, and the shear strain, γ, are given by

$$\varepsilon_C = \frac{\varepsilon_{CSA} + \varepsilon_{CSB}}{2} \tag{6}$$

$$\varepsilon_T = \frac{\varepsilon_{TSA} + \varepsilon_{TSB}}{2}$$

$$\gamma = \left|\varepsilon_C\right| + \varepsilon_T \tag{7}$$

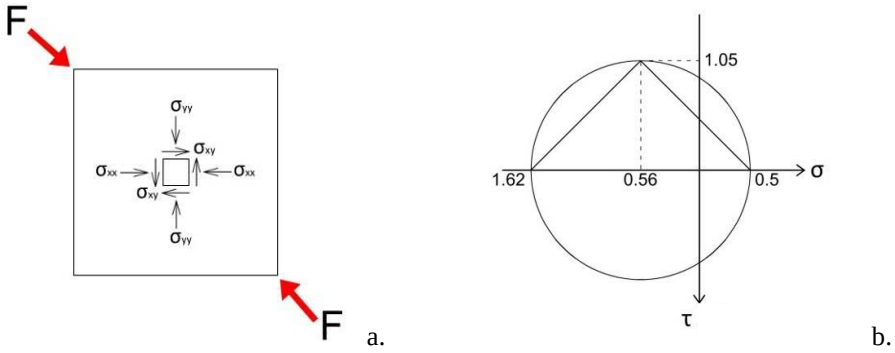

Figure 3: : a. Components of plane stress at panel centroid,
b. Graphical interpretation: Mohr's circle (tangential stress (τ), normal stress (σ)) (units in MPa).

A value of the shear stiffness modulus (G), representative of the cracked condition of the masonry, was calculated starting from the tangential stress (τ) versus angular strain (γ) curve. This was obtained by taking into account the envelope curve of the loading and unloading cycles and by constructing a bilinear curve, with a subtended equivalent-area to the tangential

stress (τ) versus angular strain (γ) curve. The equivalent bilinear curve is made of a horizontal and an inclined lines. The bilinear was calculated using the following procedure:
- The horizontal line of the bilinear was determined starting from the ultimate tension (τ_u) of the load test and ends at the ultimate angular strain (γ_u)
- By imposing energy equality, i.e. the equality between the area (A) underlying the diagram of the envelope curve and that of the bilinear equivalent, the value of the average angular deformation of the panel at the end of the inclined section of the bilinear (γ_y)

$$\gamma_y = 2\left(\gamma_u - \frac{A}{\tau_u}\right) \tag{8}$$

- The slope of the inclined line was thus obtained represents the value of the modulus of shear stiffness G (Fig. 4)

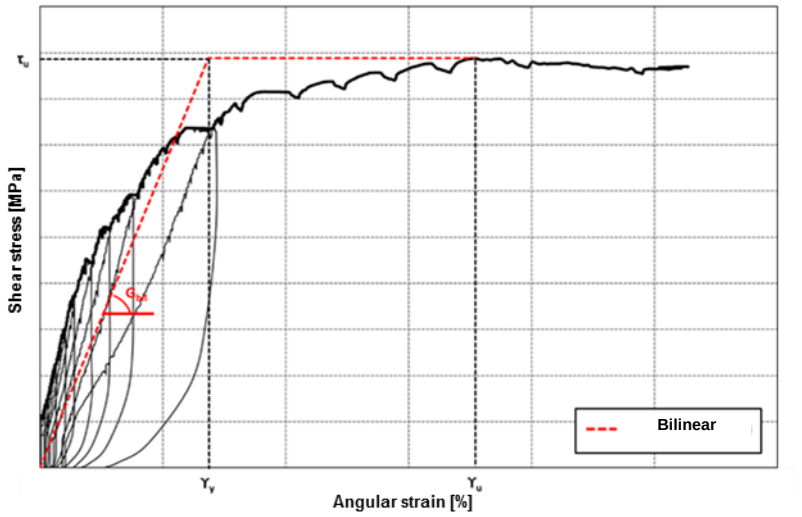

Figure 4: Determination of the shear modulus (G).

	Type of Masonry	Single- or Double side Reinforcement	Mesh Type	Coating Material
MAT-01-U	Brickwork Masonry	-	-	-
MAT-02-D		Double	1	Basic M15
MAT-03-S		Single	1	Basic M15
MAT-04-D		Double	2	Basic M15
MAT-05-S		Single	2	Basic M15
MAT-06-S		Single	1	Betonfix RCA
MAT-07-S		Single	2	Betonfix RCA
PIE-01-U	Stone Masonry	-	-	-
PIE-02-D		Double	1	Basic M15
PIE-03-S		Single	1	Basic M15
PIE-04-D		Double	2	Basic M15
PIE-05-S		Single	2	Basic M15

Table 2: Reinforcement of shear walls: test matrix.

Table 2 shows the test matrix: it can be noted that a total of twelve full-scale wall panels were tested: seven walls were made of solid bricks (MAT-series), while the remaining five (PIE-series) was constituted by ashlar (rubble) calcareous stones. The letter designations U, D and S were used to identify unreinforced, double-sided and single-sided strengthenings, respectively.

2.2 Materials and retrofitting method

A composite grid, made of fiberglass (GFRP), was applied, using an inorganic mortar, to the prepared surface of the wall panels. To connect the two coatings on the wall surfaces, composite connectors were also inserted into holes cut horizontally and transversally into the walls. The composite grids were fully embedded in the mortar coating and were secured in place by fixing them to the composite connectors. The same structural mortar used in the grid application was also employed to fill the holes.

Reinforcement application is not difficult and it can be carried on both uncracked and damaged shear walls. Furthermore, it is worth noting that the proposed retrofitting method can be used as a rapidly deployable emergency repair technique or a long-term and permanent strengthening procedure suitable for seismic protection of heritage buildings. Different methods of applying FRCM composite strengthening systems to the walls were investigated.

		Type 1	Type 2
Mesh	Material	Fiberglass, AR	Fiberglass, AR
	Weight density (dry fiber) (g/m^2)	235	465
	Weight density (pre-preg) (g/m^2)	335	581
	Mesh size (mm)	50 x 50	35 x 30
	Mesh unit uensile strength (kN/m)	63	110
Single Cord	Young's modulus (GPa)	72	72
	Elongation at Failure (%)	3.5	1.5
	Tensile strength (MPa)	1200	1200

AR = Alkali Resistant

Table 3: Two types of fiberglass mesh used for reinforcement: physical and mechanical properties.

Two types of composite grids have been used for shear reinforcement. The main mechanical properties of the GFRP meshes are listed in Table 3. These values are given in the produced data sheet (Kimia ltd., Perugia, Italy). The superficial weight density, and mesh size of Type 1 are 335 g/m^2 (for impregnated, pre-preg, fibres) and 50 x 50 mm, respectively, while higher values characterized the Type 2. A detail of the GFRP meshes are shown in Figures 5 and 6.

Two types of mortars (*Basic M15* and *Betonfix RCA*) were used for the coating (Tab. 2): Both are ready-to-use mortars, having a special fibre-reinforced composition. *Basic M15* is a lime (hydraulic) mortar and the producer (Kimia ltd.) reports in the data sheet a compressive strength > 15 MPa. On opposite *Betonfix RCA* is a cement mortar with a compressive strength > 25 MPa.

Figure 7 and Table 4 show the masonry units (brick and typical stone) and the main mechanical properties.

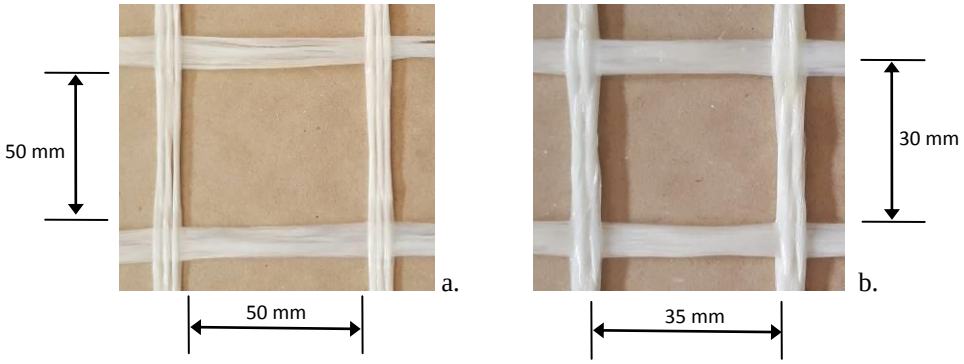

Figure 5: The two types of fiberglass mesh used for reinforcement: a. Type 1, b. Type 2

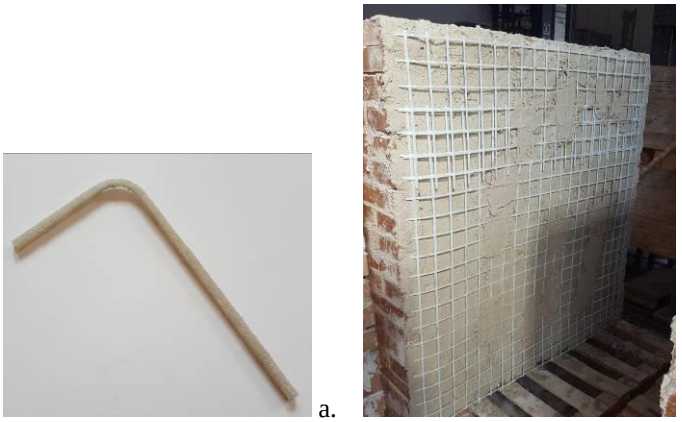

Figure 6: Reinforcement materials and application: a. Fiberglass L-shaped connectors, b. Detail of the mesh reinforcement before the application of the second layer of mortar coating.

Figure 7: a. Used materials for wall construction: Solid bricks (240 x 120 x 55 mm); b. Bonding pattern, c. Ashlar calcareous stone.

Brick	Dimensions (mm)	240 x 120 x 55
	Compressive strength (MPa)	39.00
	Bending strength (MPa)	3.61
Bedding mortar	Compressive strength (MPa)	2.69
	Bending strength (MPa)	0.76

Table 4: Bricks and mortar properties.

2.3 Test results and analysis

Table 5 shows the results in terms of the maximum load F_{max}, masonry tensile strength f_t and shear modulus. A multi-letter designation MAT has been used for brickwork panels, while this was PIE for stone work specimens. A further letter (U = unreinforced, S = single-sided reinforcement, D = double-sided reinforcement) has been adopted to specify the type of reinforcement. All GFRP-reinforcements have been applied to undamaged, sound, wall panels. Ten wall panels were reinforced (6 single-sided reinforcements, and 4 double-sided) with the GFRP grid, applied using a low-cement mortar. Panel 1 in both brickwork (MAT) and stone (PIE) series was the control panel and unreinforced.

	Wall Thickness (mm)	Single- or Double-side Reinforce-ment	F_{max} (kN)	f_t (MPa)	G (MPa)
MAT-01-U	240	-	67.03	0.077	1080
MAT-02-D	291	Double	205.0	0.236	1490
MAT-03-S	260	Single	100.3	0.117	1052
MAT-04-D	297	Double	199.8	0.233	2512
MAT-05-S	270	Single	113.4	0.133	2703
MAT-06-S	267	Single	120.9	0.141	1624
MAT-07-S	265	Single	120.9	0.138	1834
PIE-01-U	245	-	73.80	0.084	2092
PIE-02-D	303	Double	182.3	0.206	2034
PIE-03-S	285	Single	136.1	0.155	954
PIE-04-D	307	Double	209.6	0.242	876
PIE-05-S	293	Single	138.2	0.160	1902

Table 5: Results of shear tests.

For the brickwork panels, the test results show that the increase in the shear load capacity (F_{max}) is nearly three times, for double-sided reinforcement, that of the load capacity without the GFRP composite. However, for single-sided reinforcement, this increment reduced to about 70%, ranging from 49.5 % (MAT-02-D) to 80.5 % (MAT-06-S). The brickwork specimens showed the largest increase in shear capacity. The shear modulus variations were smaller in percentage and more scattered: for single-sided reinforcement, the stiffness of the wall panels increased in a range between -3.6 % and 150%.

Results from the shear tests on stone work panels are also shown in Table 5; they indicate that the average shear capacity of both single- and double-sided reinforced panels was 84 % and 164% stronger than the unreinforced wall panel.

For both brickwork and stone unreinforced panels, the shear load – angular strain curves show a quasi-elastic behaviour with a weak yield plateau: this was mainly caused by the development of a diagonal cracks along the compressed diagonal. The two unreinforced panels (denoted MAT-01-U and PIE-01-U) presented a brittle, zig-zag shaped failure along the compressed diagonal. Cracking appeared suddenly in the mortar joints and, more rarely, in the bricks, producing the instant failure of the masonry walls.

For the reinforced wall panels, shear load – angular strain curves underline two stages of the global behaviour: a first elastic and a second plastic (Figs. 8 and 9). The elastic phase of

the curves of the reinforced panels are characterized by the steeper slope as those of the unreinforced, regardless to the type of the composite reinforcement (Type 1 or Type 2). The load corresponding to the elastic limit and the ultimate load are much higher than that of unreinforced control panels. The gain in strength is quite significant. Thus, a first consequence of the reinforcement is the increase of the shear capacity of the walls. Moreover, it can be also noted an important increase of the post-elastic deformation capability of the reinforced walls, emphasized by the presence of a relevant post-elastic plateau. Because tests were conducted in load stroke-control (and not displacement-control) this is a pseudo-ductility and reader should be alerted about the limitations of the post-peak test data. Figure 10 shows the typical failure modes on both unreinforced and reinforced wall panels.

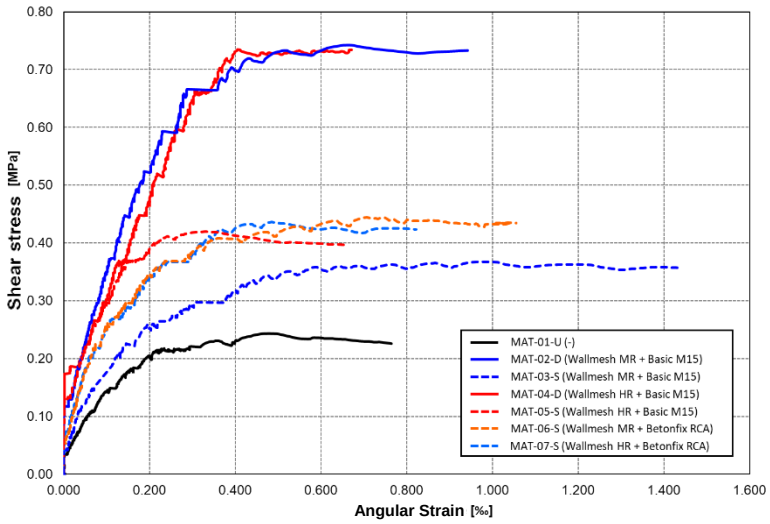

Figure 8: Envelope of the shear stress (τ) versus angular strain (γ) curves for the brickwork panels.

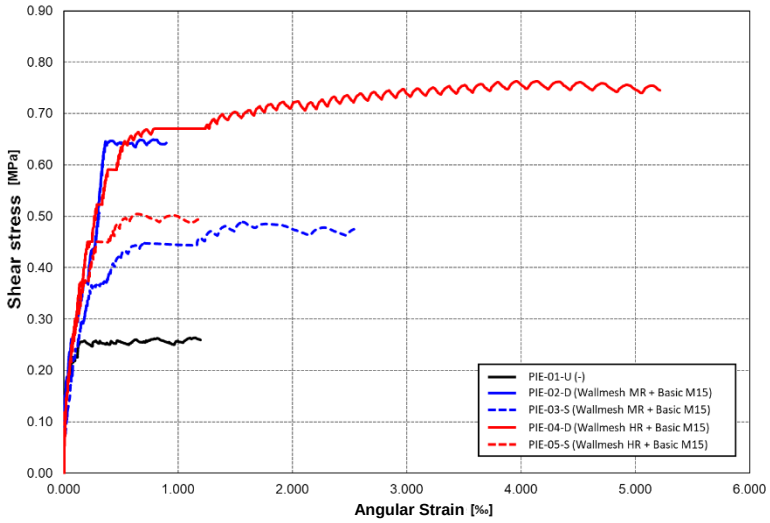

Figure 9: Envelope of the shear stress (τ) versus angular strain (γ) curves for the stone panels.

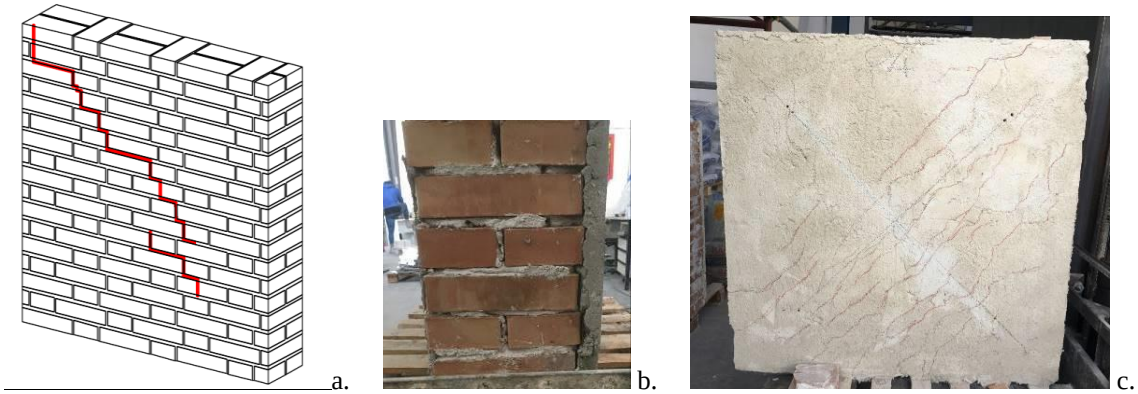

a. b. c.

Figure 10: Failure modes: a. Unreinforced brickwork panel, b. Single-sided reinforced brickwork specimens, c. Shear cracks on the double-sided reinforced wall.

3 NUMERICAL SIMULATION

3.1 FE model

The experimental data were implemented numerically, via non-linear constitutive laws, in a commercial FE modelling code. Accounting for the brickwork masonry nonlinear behavior [14, 15, 16], 3D finite element (FE) models were thus adopted. To this end, after defining their geometry with CAD drawings, the panels were discretized by means of iso-parametric solid elements (Solid 65), having 8 nodes with 3 Degrees of Freedom (DOF) at each node. To facilitate the analysis, the periodically repeating patterns of the brick masonry typology was modelled by dividing each periodic unit cell into ten cuboid subcells (ten brick units, three head and one bed joints) characterized by different material properties (Figure 11).

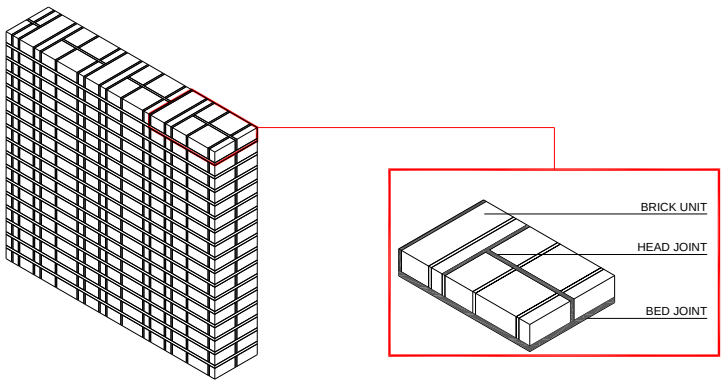

Figure 11: Derivation of periodic unit cell.

Since all units were identically oriented and the masonry layout did not change through the thickness, for convergence checking, each periodic unit cell was then modelled with a sufficient number of elements through the height of each sub-cell. After performing a sensitivity analysis varying the mesh size, the mesh of all FE models was thus refined so as to have three elements (18.33 × 20 × 20 mm) across each brick unit, two elements (18.33 × 20 × 3.33 mm) across each bed joint and a single element (7 × 20 × 20 mm) across each head joint (it is important to remark that in this two latter cases the size of the mesh was dictated by the thickness of the mortar joints).

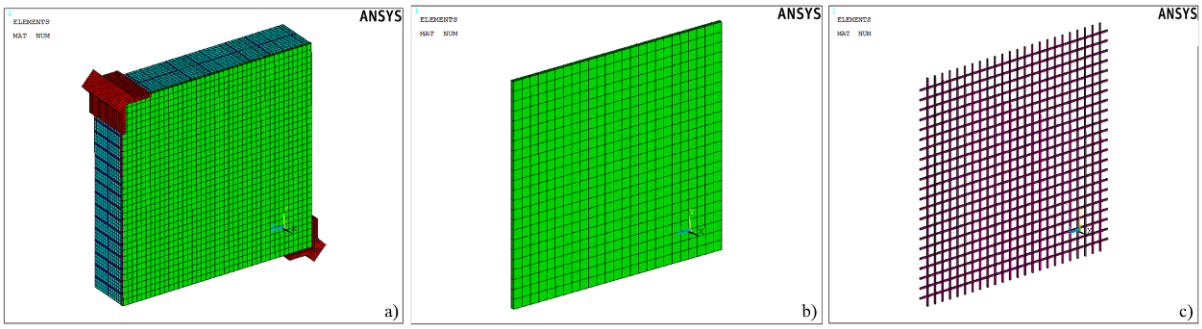

Figure 12: FE model with mesh discretization: a. Reinforced model; b. Mortar coating; c. GFRP mesh.

As for reinforcement, a shared node approach was instead used for simulating the GFRP meshes embedded into the mortar coating. Accordingly, the connection between the mortar matrix and the reinforcement was achieved treating the glass meshes (modelled by means of 2-noded uniaxial tension-compression Link 180 elements) as a slave material, which is merged to the surrounding master material.

This allows to capture the more critical details avoiding distorted meshes as well as shear lock effects. Figure 12 shows the full FE model, which is characterized by 85,642 elements and 90,356 nodes, with 271,068 DOF.

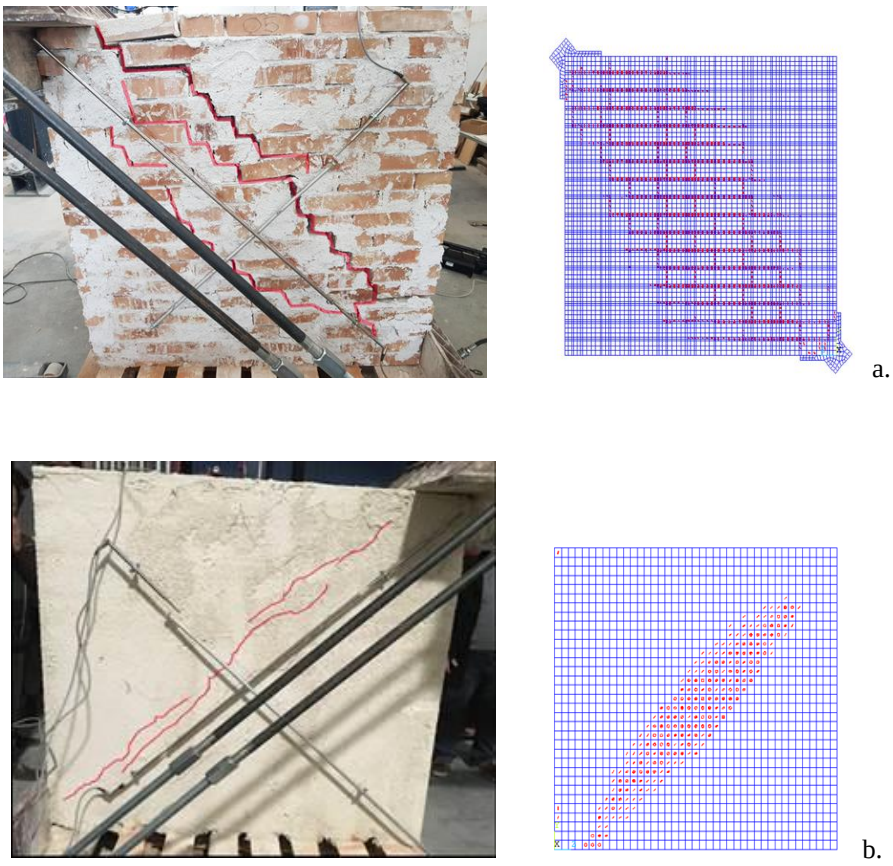

Figure 13. Experimental vs FE model crack pattern: a. Unreinforced face; b. Reinforced face.

To model the behavior of brickwork masonry, a 3d nonlinear analysis was implemented through the use of a damage mechanic approach. Based on this, a tensile cut-off failure criterion was adopted for each masonry component (brick units, bead and head joints). The aforementioned elastic-plastic model, generally used for brittle materials such as concrete, can account for either crushing or cracking failure modes using a smeared model. More specifically, the cracking pattern observed during the damaging process of both bricks and mortar joints was simulated by means of only 2 material parameters (assigned according to the material properties obtained through the experimental tests): compressive (f_c) and tensile (f_t) strength. Moreover, to increase the reliability of the proposed analysis, the simulation of the contacts between the panel and loading plates was performed using unilateral contact interfaces. Accordingly, surface-to-surface contact elements were adopted, determining the contacting properties for the tangent and normal behavior through the use of a trial-and-error procedure. In detail, a Coulomb friction law was used assuming that at each interface sliding may (or may not) occur by introducing a coefficient of friction ($\mu = 0.3$).

3.2 FEA results

According to the aim of simulating the in-plane response of the specimens and therefore providing an interpretation of the detected damage pattern, FE analyses were developed, in which each model was firstly subjected to self-weight, followed by a ramped 9000 N shear load. Figure 13 reports the cracking pattern observed during the FE analysis on the panels. In agreement with the damage observed at the end of the experimental tests, cracking is not present on the whole panel, but mainly on its bed and head joints. More specifically, following predominant horizontal cracking initiated at the specimen mid-height, when the interface bond strength was attained, stepped diagonal cracks spread (through horizontal and vertical joints) along the compressed diagonal.

As shown in Table 6, in order to evaluate the efficiency and accuracy of the proposed FEM, the estimates of the ultimate shear capacity were then compared with laboratory outcomes. Even in this case, it can be emphasized how FE models satisfactorily reproduce the observed ultimate capacities, since in all cases the maximum deviations between predicted and measured response (i.e., error of the model) were found to be no more than 14%.

	Predicted in-plane capacity (kN)	Experimental in-plane capacity (kN)	Error of the model (-)
MAT-01-U	67.5	67.03	1.01
MAT-02-D	176.25	205.0	0.86
MAT-03-S	112.5	100.3	1.12
MAT-04-D	172.5	199.8	0.86
MAT-05-S	112.5	113.4	0.99
MAT-06-S	135	120.9	1.12
MAT-07-S	135	120.9	1.12

Table 6. Experimental vs predicted shear load capacities.

4 CONCLUSIONS

This research has investigated the shear behavior of stone and brickwork masonry walls, strengthened using GFRP meshes embedded into a mortar coating. Full-scale shear tests and numerical simulations were performed to determine the strength capacity of wall panels reinforced with the proposed retrofitting method.

The following conclusions can be drawn:

- brickwork panels, test results show that the increase in the shear load capacity, for double-sided reinforcement, is nearly three times higher than the shear capacity of unreinforced wall panels. For single-sided reinforcement, this increment reduced to about 70 %, ranging from 49.5 % to 80.5 %. The brickwork specimens showed the largest increase in shear capacity. The shear modulus variations were smaller in percentage and more scattered: for single-sided reinforcement, the stiffness of the wall panels increased in a range between -3.6 % and 150 %.

- Stone work panels, they indicate that the average shear capacity of both single- and double-sided reinforced panels was 84 % and 164 % stronger than the unreinforced wall panel.

- For both brickwork and stone unreinforced panels, the shear load – angular strain curves showed a quasi-elastic behaviour with a weak yield plateau: this was mainly caused by the development of a diagonal shear crack along the compressed diagonal. For the reinforced panels, shear load – angular strain curves underline two stages of the global behaviour: a first elastic and a second plastic.

- Although the number of tested panels was limited and not exhaustive, we can remark that the reinforcement caused a significant increase of the ultimate strength of the panels; the typical failure mode was due to masonry crushing.

- Furthermore, this initial attempt to model the GFRP-reinforced wall panels, while not complete, demonstrates that structural modeling is possible given accurate information on material property evolution and structural response of both unreinforced and reinforced panels. In addition, we require a better understanding of boundary conditions at interface coating-to-masonry. As we continue this part of the program we wish to develop further examples and isolate those details that are critical to making accurate predictions. The experimental data were implemented numerically using a non-linear constitutive law and adopting a 3D finite element model. The results of the numerical analysis are in agreement with the observations of the experimental tests: unit (stone or bricks) cracking was not noted, but failure mainly occurred at the bed and head joints. Moreover, the numerical ultimate shear capacity was then compared with laboratory results in order to evaluate the efficiency and accuracy of the proposed FEM. Considering that the maximum error of the numerical simulation was 14 %, it can be highlighted that FE model satisfactorily reproduced the observed experimental ultimate capacities.

REFERENCES

[1] S. Boschi, L. Galano, V. Vignoli, Mechanical characterisation of Tuscany masonry typologies by in situ tests, *Bulletin of Earthquake Engineering*, 17(1), 413-38, 2019.

[2] M. Corradi. A. Borri, A database of the structural behavior of masonry in shear, *ulletin of Earthquake Engineering*, 9, 3905-30, 2018.

[3] G. Castori, A. Borri, A. De Maria, M. Corradi, R. Sisti, Seismic vulnerability assessment of a monumental masonry building, *Engineering Structures*, 136, 454-465, 2017.

[4] Y. Boffill, H. Blanco, I. Lombillo, L. Villegas, Assessment of historic brickwork under compression and comparison with available equations. *Construction and Building Materials*, 207, 258-272, 2019.

[5] M. Corradi, A. Borri, G. Castori, R. Sisti, The Reticulatus method for shear strengthening of fair-faced masonry, *Bulletin of Earthquake Engineering*, 14(12). 3547-3571, 2016.

[6] A. Borri, M. Corradi, A. Vignoli, Seismic upgrading of masonry structures with FRP. Proceeding of 7th International Conference on inspection appraisal repairs and maintenance of buildings and structures, Nottingham, UK, 2001

[7] R. Capozucca, Experimental analysis of historic masonry walls reinforced by CFRP under in-plane cyclic loading. *Composite Structures*, 94 (1), 277-289, 2011.

[8] T. Stratford, G. Pascale, O. Manfroni, B. Bonfiglioli, Shear strengthening masonry panels with sheet glass-fiber reinforced polymer. *Journal of Composites for Construction*, 8(5), 434-443, 2004.

[9] T.C. Triantafillou, Strengthening of masonry structures using epoxy-bonded FRP laminates. *Journal of Composites for Construction*, 2, 96-104, 1998.

[10] ICOMOS Charter, Principles for the analysis, conservation and structural restoration of architectural heritage. ICOMOS 14th General Assembly and Scientific Symposium, Victoria Falls, 2003, Zimbabwe.

[11] T.C. Triantafillou, C.G. Papanicolaou, Shear strengthening of reinforced concrete members with textile reinforced mortar (TRM) jackets. *Materials and structures*, 39(1), 93-103, 2006.

[12] F.G. Carozzi, G. Milani, C. Poggi, Mechanical properties and numerical modeling of Fabric Reinforced Cementitious Matrix (FRCM) systems for strengthening of masonry structures. *Composite structures*, 107, 711-725, 2014.

[13] S. Casacci, C. Gentilini, A. Di Tommaso, D.V. Oliveira, Shear strengthening of masonry wallettes resorting to structural repointing and FRCM composites. *Construction and Building Materials*, 206, 19-34, 2019.

[14] P.B. Lourenço, J.T. Rots, J. Blaauwendraad, Two approaches for the analysis of masonry structures: micro and macro-modeling, *Heron*, 40(4), 313-340, 1995.

[15] D. Addessi, S. Marfia, E. Sacco, J. Toti, Modeling approaches for masonry structures, *Open Civil Engineering Journal*, 8, 288-300, 2014.

[16] V. Sarhosis, J.V. Lemos, A detailed micro-modelling approach for the structural analysis of masonry assemblages, *Computers and Structures*, 206, 66-81, 2018.

[17] M. Betti, L. Galano, A. Vignoli, Finite element modelling for seismic assessment of historic masonry buildings, Earthquakes and their impact on society. Earthquakes and Their Impact on Society. Springer, Berlin, 2016.